Plant Physiology and Biochemistry 135 (2019) 588–600

Contents lists available at ScienceDirect

Plant Physiology and Biochemistry

journal homepage: www.elsevier.com/locate/plaphy

Research article

AQUA1 is a mercury sensitive poplar aquaporin regulated at transcriptional and post-translational levels by Zn stress

Andrea Ariani[a,1], Fabrizio Barozzi[b], Luca Sebastiani[a], Luigi Sanità di Toppi[c], Gian Pietro di Sansebastiano[b], Andrea Andreucci[c,*]

[a] BioLabs, Institute of Life Sciences, Scuola Superiore Sant'Anna, Pisa, Italy
[b] DISTEBA, Department of Biological and Environmental Sciences and Technologies, University of Salento, Via Prov. le Lecce – Monteroni, 73100, Lecce, Italy
[c] Department of Biology, Università degli Studi di Pisa, I-56126, Pisa, Italy

ARTICLE INFO

Keywords:
Aquaporins
Phytoremediation
Populus x canadensis
Post-translation modification
Zn stress

ABSTRACT

Aquaporins are water channel proteins that regulate plant development, growth, and response to environmental stresses. *Populus trichocarpa* is one of the plants with the highest number of aquaporins in its genome, but only few of them have been characterized at the whole plant functional level. Here we analyzed a putative aquaporin gene, *aqua1*, a gene that encodes for a protein of 257 amino acid with the typical NPA (Asp-Pro-Ala) signature motif of the aquaporin gene family. *aqua1* was down-regulated of ~10 fold under excess Zn in both leaves and roots, and conferred Zn tolerance when expressed in yeast Zn hypersensitive strain. *In vivo* localization of AQUA1-GFP in *Arabidopsis* protoplast showed a heterogeneous distribution of this protein on different membranes destined to form aggregates related to autophagic multivesicular bodies. Zn-dependent AQUA1-GFP re-localization was perturbed by phosphatases' and kinases' inhibitors that could affect both intracellular trafficking and aquaporins' activity. Exposed to high concentration of Zn, AQUA1 also co-localized with AtTIP1;1, a well-known *Arabidopsis* vacuolar marker, probably in pro-vacuolar multivesicular bodies. These findings suggest that high concentration of Zn down-regulates *aqua1* and causes its re-localization in new forming pro-vacuoles. This Zn-dependent re-localization appears to be mediated by mechanisms regulating intracellular trafficking and aquaporins' post-translational modifications. This functional characterization of a poplar aquaporin in response to excess Zn will be a useful reference for understanding aquaporins' roles and regulation in response to high concentration of Zn in poplar.

1. Introduction

Heavy metal contamination derived from urban activities, agricultural operations and industrial processing constitute a worldwide problem nowadays (Lado et al., 2008; Li et al., 2001). Zinc (Zn) is one of the most common contaminants (http://eusoils.jrc.ec.europa.eu/foregshmc/) with toxic Zn concentrations for plants occurring in soils (especially at low pH) contaminated by mining and smelting activities, sewage sludge, and other human-relate activities (Broadley et al., 2007).

Endemic plants of areas with elevated metal contamination, like the hyperaccumulator *Noccaea caerulescens* and *Arabidopsis halleri*, are able to accumulate more than 1% of their dry biomass in Cd and Zn, 10 times more than non-accumulator plants (Rigola et al., 2006; Zhao et al., 2000). This natural metal uptake capacity suggested the use of hyperaccumulator plants in phytoremediation programs, even if they have low growth rate and a poor biomass production. On the other hand, high biomass-producing perennial plants like trees could be a valuable alternative to these hyperaccumulator plants (Pulford and Dickinson, 2005). Species from the *Salicacea* family could be useful for phytoremediation application thanks to their high growth rate, biomass production, tolerance to heavy metal, and also thanks to their adaptation to wetland systems (Kuzovkina and Quigley, 2005; Mertens et al., 2006; Pulford et al., 2001; Tack et al., 2005). In particular, *Populus* species and hybrids have been used in studies on heavy metal tolerance and phytoremediation programs (Castiglione et al., 2009; Dos Santos Utmazian et al., 2007; Laureysens et al., 2005; Pulford and Dickinson, 2005; Sebastiani et al., 2004; Tognetti et al., 2004). In addition, the availability of a full annotated genome sequence of *Populus trichocarpa* makes this species the model plant for tree-specific physiological and

* Corresponding author. Department of Biology, Via L. Ghini, 13, I-56126, Pisa, Italy.
E-mail address: andrea.andreucci@unipi.it (A. Andreucci).
[1] Present address: BASF Agricultural Solutions Belgium NV, Technologiepark 38, 9052, Ghent, Belgium.

https://doi.org/10.1016/j.plaphy.2018.10.038
Received 30 July 2018; Received in revised form 30 October 2018; Accepted 30 October 2018
Available online 02 November 2018

molecular studies (Tuskan et al., 2006). Several of the biochemical mechanisms essential for heavy metal tolerance and accumulation are well known in plant (Li et al., 2018; Singh et al., 2015; Zhu, 2016), but the molecular events underlying heavy metal sensing, signal transduction and defense systems have been only partially elucidated. In previous studies, the hybrid poplar clone I-214 (*Populus x canadensis* Moench) was extensively used as a model system for elucidating molecular, physiological, biochemical and anatomical responses to excess Zn (Di Baccio et al., 2010, 2003; Di Baccio et al., 2009; Stoláriková et al., 2012). In particular, high throughput analyses performed in leaf and root under Zn stress identifies several differentially expressed genes, like those involved in glutathione metabolisms, ion homeostasis and water transport, such as aquaporins (Ariani et al., 2015; Di Baccio et al., 2011).

Aquaporins are small membranes proteins ubiquitous in all organisms (Gomes et al., 2009), and several studies report that in addition to water, aquaporins can transport other substrates of great physiological interest such as ammonia, boron, carbon dioxide, hydrogen peroxide, silicon and urea (Hove and Bhave, 2011; Maurel et al., 2008), proving to be more than simple water channels and possibly engaged in structural roles (Chevalier and Chaumont, 2015; Hachez et al., 2014a, 2014b).

Despite the evolutionary differences between aquaporins, the typical protein structure was highly conserved with a tetrameric quaternary structure characterized by a central aqueous pore carrying the conserved NPA motif (Asp-Pro-Ala) specific of aquaporins (Danielson and Johanson, 2008; Li et al., 2014). Furthermore, the majority of aquaporins share conserved Cys residues which determines sensitivity towards $HgCl_2$ (Li et al., 2014) that can block the pore by directly binding to this site, and a reducing agent, i.e. DTT, could revert this inhibition (Hirano et al., 2010). These characteristics have been extensively used for aquaporin identification and for evaluation of aquaporin-mediated water-flow across different tissues (Javot and Maurel, 2002).

Aquaporins are a large and highly divergent protein super-family in plants, with more than thirty members identified in *Arabidopsis thaliana* (Johanson et al., 2001; Quigley et al., 2002), *Zea mays* (Chaumont et al., 2001), *Oryza sativa* (Sakurai et al., 2005) and *Populus trichocarpa* (Gupta and Sankararamakrishnan, 2009). Plant aquaporins are usually classified into four subfamilies based on sequence homology and subcellular localization. These subfamilies are: plasma membrane intrinsic proteins (PIP), with two groups (PIP1 and PIP2); tonoplastic intrinsic proteins (TIP); nodulin 26-like intrinsic proteins (NIPs) and small intrinsic proteins (SIPs) (Li et al., 2014).

Aquaporins are tightly regulated by an integrated signaling network at both transcriptional and post-transductionaltranslational level (Maurel et al., 2008) and their water-flow activity can also be modulated by direct gating of protons and divalent cations (Gerbeau et al., 2002) and heterotetramerization among isoforms (Chaumont et al., 2005; Li et al., 2014). Aquaporin phosphorylation occurs in interdependent sites at both N− and C-terminal part of the proteins (Boursiac et al., 2008; Chaumont et al., 2005) that can directly gate the channel (Chevalier and Chaumont, 2015; Horie et al., 2011) or affect protein's re-localization (Chevalier and Chaumont, 2015; Li et al., 2014; Prak et al., 2008). Moreover, aquaporins were also subjected to co-translational maturation process of their N-terminus by N-α-acetylation of specific residue, cleavage of initiating methionine or methylation of two adjacent sites of the protein. These modifications may regulate the correct export of the protein to the plasma membrane and determine their stability (Santoni et al., 2006). Finally, several studies report that aquaporins can undergo modifications, such glycosylation (Vera-Estrella et al., 2004) or ubiquitination (Lee et al., 2009), which accompany a stress-induced or development-induced re-localization.

Previous analysis of a *Populus x canadensis* aquaporin (*aqua1*, GenBank: GQ918138) in transgenic *Populus* plants showed a stomata specific localization of this protein, but transgenic over expressing lines did not show any differences in comparison to wild type plants regarding stomatal conductance and photosynthetic activity (Ariani et al., 2016). These results suggested possible modifications of *aqua1* activity by regulation of cellular localization or post-translational modification of this gene. For testing these hypotheses, we analyzed the function and regulation of this gene at both transcriptional, sub-cellular, and post-translational level in response to excess Zn. To our knowledge, this is the first functional characterization of a *Populus* aquaporin in response to excess Zn.

2. Materials and methods

2.1. Poplar growing conditions

Woody cuttings of the hybrid poplar *P x canadensis* Moench clone I-214 were provided by the Istituto Sperimentale per la Pioppicoltura (Casale Monferrato, Italy).

After rooting, woody cuttings were transplanted into plastic pots with Agrileca clay (Laterlite, Milano, Italy) and grown in a controlled growth chamber under an hydroponic system. Aeration of nutrient solution ($250\,L\,h^{-1}$) was applied using aquarium air pumps. Growth conditions were as follow: 23-18 °C day-night temperature, 65–70% relative humidity and a photoperiod of 16/8 h light/dark at a maximum photon flux density of $400\,\mu mol\,m^{-2}\,s^{-1}$ (photosynthetically active radiation) supplied by fluorescent lights.

Plant growth and Zn screening were performed in a hydroponic system using two different Zn treatments: (i) basic Hoagland's solution with 1 μM Zn (0.065 ppm, i.e., the control); (ii) basic Hoagland's solution with 1 mM Zn (65 ppm) as previously described in Di Baccio et al. (2011).

2.2. Arabidopsis growing and transient transformation conditions

Arabidopsis thaliana (ecotype Colombia 0) seeds were sterilized by washes in 10% household bleach (0.45% sodium hypochlorite at final concentration) for 1 min and in ethanol 70% for 1 min. Seeds were then collected and washed with abundant bi-distilled sterile water. The seeds were sown on MS medium (Duchefa) as described by Li et al. (2009) and germinated at 21 °C with a photoperiod 16 h/8 h light dark. Four days after germination, the plantlets were agroinfiltrated with *Agrobacterium tumefaciens* GV3101 according to Li et al. (2009) with minor modifications. *A. tumefaciens* was grown in LB and in presence of rifampicin ($50\,\mu g\,ml^{-1}$), gentamycin ($25\,\mu g\,ml^{-1}$), as well as the antibiotic for binary plasmid. After 24 h from co-cultivation start, the agrobacterium suspension was eliminated washing plants with MS medium. The plants were incubated again in the dark and observed by confocal microscopy after 48 h from transformation.

2.3. Cloning of aqua1

The CDS of *aqua1* was amplified by RT–PCR on mRNA isolated from I-214 poplar leaves, and cloned into the pCRII vector (Invitrogen). The reverse transcription reaction was performed using the QuantiTect Reverse Transcription Kit (Qiagen, http://www.qiagen.com) in accordance with the manufacturer's manual. The cDNA obtained was then amplified with PCR using the Phusion High-Fidelity DNA polymerase (Finnzymes, http://www.finnzymes.com) and the primers coupled with the following oligonucleotides derived from the putative 5′- and 3′-UTR of the homologue *Populus trichocarpa* aquaporin gene: forward TAGG TACATCCGGGAGTG, reverse ACAACGAATCCAACGTAGTC. The *aqua1* product of this amplification was directly ligated, after A-tailing, to the pCRII vector, using the TA Cloning Kit Dual Promoter (Invitrogen, http://www.invitrogen.com) in accordance with the manufacturer's manual. All the clones were sequenced by PRIMM company, Italy. The *aqua1* sequence has been deposited in PubMed database (GenBank: GQ918138.1).

The *aqua1* genomic sequence was amplified by PCR from genomic DNA isolated from poplar I-214 clone leaves using the ChargeSwitch gDNA Plant Kit (Invitrogen). The DNA was used as template for the PCR reactions, which were performed as above using the primers designed over the cDNA sequence (forward: ATGCGTAATTTTATTACATCGAAC; reverse: CTAAAACTCCTCCACCGGGCA). The cloning and the sequencing procedures were performed as above.

2.4. Genomic DNA and mRNA extraction

The extraction of both genomic DNA and total mRNA was performed from 80 to 100 mg leaf or root tissue flash frozen in liquid nitrogen and kept at −80 °C. DNA/RNA extractions were performed using respectively the DNeasy plant mini kit (Qiagen) and RNeasy plant mini kit (Qiagen) according to manufacturer's instructions. Genomic DNA was removed from total RNA prior to reverse transcription by digesting the samples with the RNase Free DNase set (Qiagen).

2.5. mRNA relative quantification

Real time PCR of *aqua1* expression were performed as previously described (Ariani et al., 2016). In brief, RNA concentration and quality were evaluated using the Experion RNA StdSens Kit (Biorad). One μg of total RNA was reverse transcribed using the Quantitect Reverse Transcription Kit (Qiagen) according to manufacturer's instructions. Real-time PCR were performed with Quantitect SYBR Green PCR Kit (Qiagen) according to manufacturer's instructions on the ECO Real-Time PCR System (Illumina Inc. San Diego, USA). For *aqua1* amplification we used the following primers: forward 5′CCTCCGTGGCATTCT GTATT3′, reverse 5′CAAAGGTCCAGCCCAGTAAA3'. As reference genes we used β-tubulin for leaves, and EF1α for root from Brunner et al. (2004) Relative gene expression levels were calculated with the $2^{-\Delta\Delta Ct}$ method (Livak and Schmittgen, 2001). Each PCR analysis was repeated three times for three different biological replicates.

2.6. Constructs preparation for confocal analysis

The fusion construct for AQUA1-GFP was generated by PCR amplification of the cDNA with specific forward (5′) and reverse (3′) primers containing anchored BglII and XbaI restriction sites, respectively. The PCR products were ligated into the pCRII vector and sequenced. The amplified insert was excised after digestion with BglII and XbaI restriction enzymes (NEB, https://www.neb.com/) and ligated in plant-specific expression vector pAVA393 GFP (Dr. von Arnim's gift).

Open reading frames of *PtAQUA1*, At*SYP122*, At*SYP51, AtATG8f,* the first 53 amino acids of the sialyltransferase of *Rattus norvegicus* (ST) derived from the chimeric protein ST-RFP (Saint-Jore-Dupas et al., 2006), Cherry-BP80 (S1) and RFP-KDEL were amplified with specific primers (S2) including Gateway attachment sites (attB1/attB2).

A subsequent BP reaction in pDONR221 (Invitrogen) yielded Entry clones that were verified via sequencing. To generate the final construct, each Entry clone was made react with an appropriate pDest vector trough LR reaction (Invitrogen). For *AQUA1* was used the pDest pK7FWG2 (C-terminal fusion GFP), for *SYP122*, *SYP51* and*ATG8f* the pDEST pH7WGR2 (N-terminal fusion RFP), for ST the pDEST pK7RWG2 (C-terminal fusion RFP) the and for Cherry-BP80 and RFP-KDEL the pDEST pK2GW7 that doesn't contain any fluorescent tag. The expression of the constructs produced was expected to reproduce published data, labelling respectively PM with RFP:AtSYP122 (Rehman et al., 2008), TGN and tonoplast with RFP:AtSYP51 (De Benedictis et al., 2013), RFP-ATG8f in autophagosomes (Michaeli et al., 2014), ER with RFP-KDEL (Nesler et al., 2017), PVC with Cherry-BP80 (De Benedictis et al., 2013).

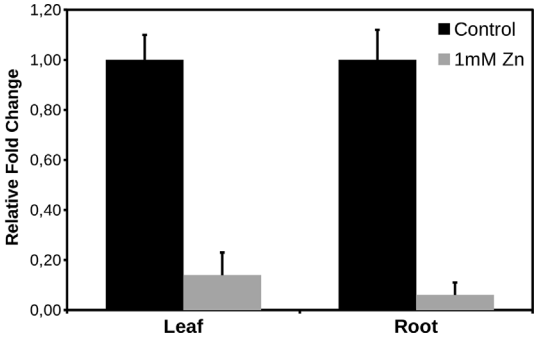

Fig. 1. *aqua1* differential expression in response to excess Zn in leaf and root tissues. Differential expression of *aqua1* in leaves and roots in control condition and exposed to 1 mM of Zn (Zn). The expression levels were indicated as relative fold change using the $2^{-\Delta\Delta Ct}$ method. β-tubulin and EF1α were used as reference genes in leaf and root tissues, respectively. Each data and the corresponding error bar represent average and standard deviation of three biological replicates, respectively.

2.7. Transient expression studies in Arabidopsis protoplast

Protoplasts used for fluorescent proteins localization were isolated from 5 weeks old plant rosettes and transformed as previously described (De Benedictis et al., 2013).

Protoplasts used for chemical treatments were isolated from 3-day-old *Arabidopsis* cell suspension cultures as described in Scebba et al. (2003) and transient transfections were carried out by Gene Pulser Xcell electroporation system (BioRad, http://www.biorad.com) (Pitto et al., 2000). After electroporation, the protoplasts were grown on modified MS medium (MS, 3% sucrose, 0.3 M mannitol, 0.1 mg l^{-1} 2,4 D, 0.2 mg l^{-1} 6-BAP, 10^{-6} M α-NAA, pH 5.8).

To study the Zn effects on AQUA1 localization, after transfection 100 μM and 200 μM $Zn(NO_3)_2$ $6H_2O$ (LD_{50} and LD_{70}, respectively) were added to the culture medium and the cells were analyzed on confocal microscope after 24 h.

For inhibition of AQUA1 activity, after transfection the culture medium was supplemented with 10 μM $HgCl_2$ and 200 μM $Zn(NO_3)_2$ $6H_2O$. The cells were cultured for 24 h before the confocal microscopy observation. To test the recovery of Hg induced reduction in AQUA1 activity, a new AQUA1 transfection experiment was exposed first to 10 μM $HgCl_2$ for 24 h and then, to 100 mM DTT for other 24 h. To remove the $HgCl_2$, the suspension cells were centrifuged twice at 2000 × *g* for 5 min and the cell pellets re-suspended in fresh culture medium before adding DTT. Confocal images analysis has been performed 24 h and 48 h after electroporation. Cell viability test with the above mentioned $HgCl_2$ and DTT concentrations has been performed with fluorescein diacetate (FDA) prior to transfection experiments and sub-cellular localization analyses.

To check the effect of inhibition of phosphatase and kinase activities on AQUA1 trafficking, wortmannin (Wt) and okadaic acid (OA) were added to the culture medium supplemented with 200 μM $Zn(NO_3)_2$ $6H_2O$ after electroporation and analyzed in different experimental conditions. The concentration of 0.01, 0.1, 1 and 3 μM OA acid and 2 and 10 μM Wt have been used for 24 h before confocal observations.

2.8. aqua1 expression in yeast

aqua1 coding sequence was excised from pCRII after digestion with EcoRI and XbaI restriction enzymes (NEB) and ligated into the pYES2 yeast expressing vector (Invitrogen). The yeast strain BY4741 (Schiestl and Petes, 1991) and the double mutant strain (*zrc1cot1*) (MacDiarmid et al., 2003) were transformed with the lithium acetate method (Gietz et al., 1995). The transformants were selected on high-stringency synthetic medium lacking uracile (SD). For metal tolerance assays, yeast

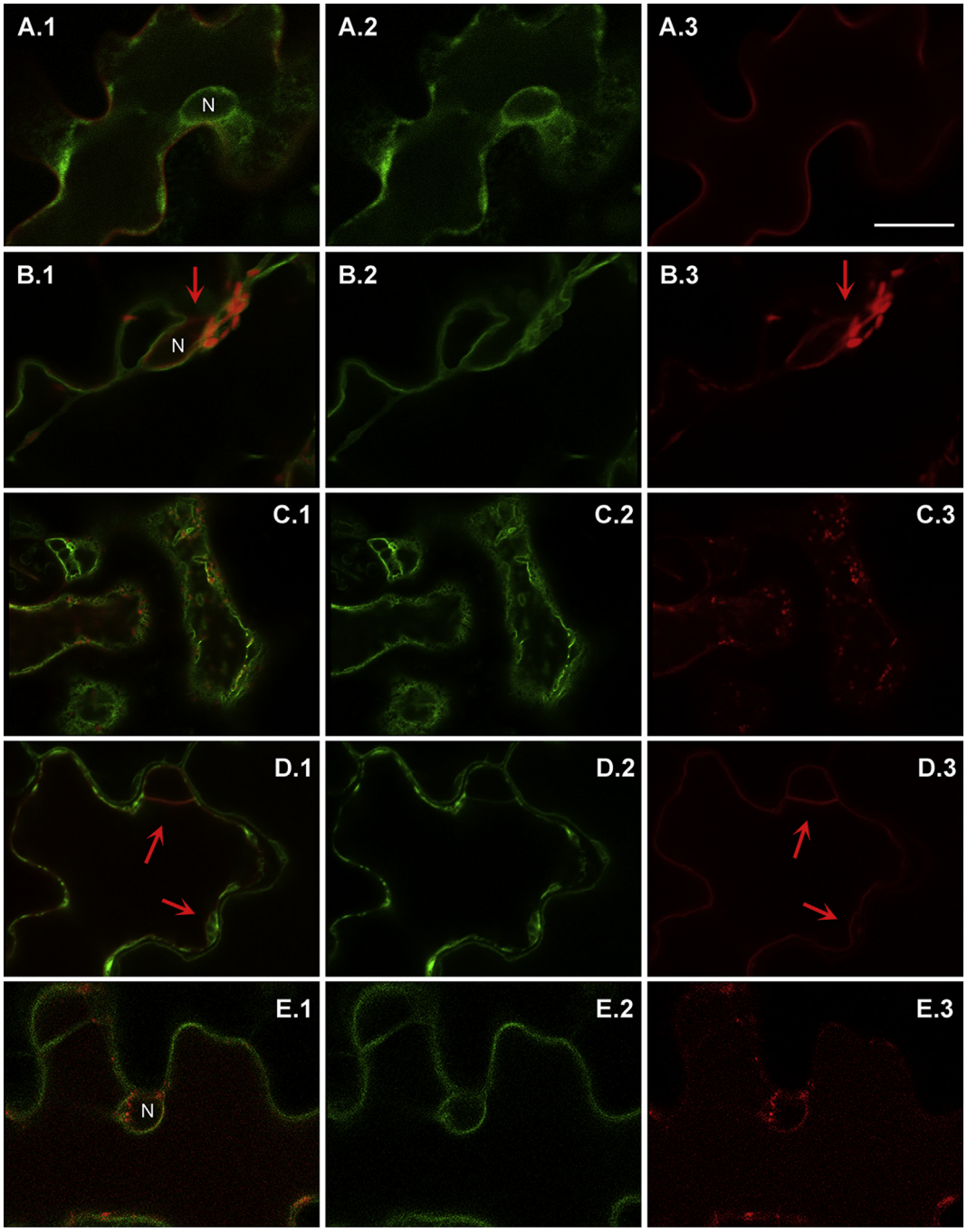

Fig. 2. Co-expression of AQUA1-GFP with A) PM marker RFP-SYP122; B) ER marker RFP-KDEL; the arrow evidences the red labeling of nuclear envelop in an area not co-labeled by AQUA1-GFP. C) Golgi marker STRFP; D) Tonoplast marker RFP-SYP51; arrows evidence areas where tonoplast is well visible. E) PVC marker Cherry-BP80. "N" indicates the position of the nucleus. Scale bar 10 μm. (For interpretation of the references to color in this figure legend, the reader is referred to the Web version of this article.)

was grown on SD medium to an OD_{600} of 1 to perform further dilutions. The drop assays were performed with three different yeast transformants on SD plates with and without 5% galactose containing 0 μM, 10 μM, 50 μM, 100 μM and 200 μM $Zn(NO_3)_2{\cdot}6H_2O$. As control pYES2 empty vector was used and the transformants were processed together with pYES2-AQUA1.

2.9. Confocal imaging

The fluorescent protein distribution in protoplasts and transgenic plants was examined using a confocal laser-scanning microscope LSM 710 Zeiss (ZEN Software, GmbH, Germany). GFP markers were detected in the wavelength range 505–530 nm (green color); RFP and Cherry markers were detected in the wavelength range 560–600 nm (red color); chlorophyll epifluorescence was detected above 650 nm (blue color). Excitation wavelength of 488 and 543 nm were used simultaneously. Images were processed using Adobe Photoshop 7.0 software (Mountain View, CA, USA).

The transformed protoplasts expressing AQUA1-GFP under different treatments were analyzed with an inverted Leica TCS SP2 confocal laser scanning microscope (Leica Microsystems, http://www.leica.com), using a 63X NA 1.3 Plan-Apo oil-immersion objective at 1024 × 1024 pixel resolution. For GFP fluorescence analyses, we used the 488 nm excitation line of an argon ion laser and the emission light was

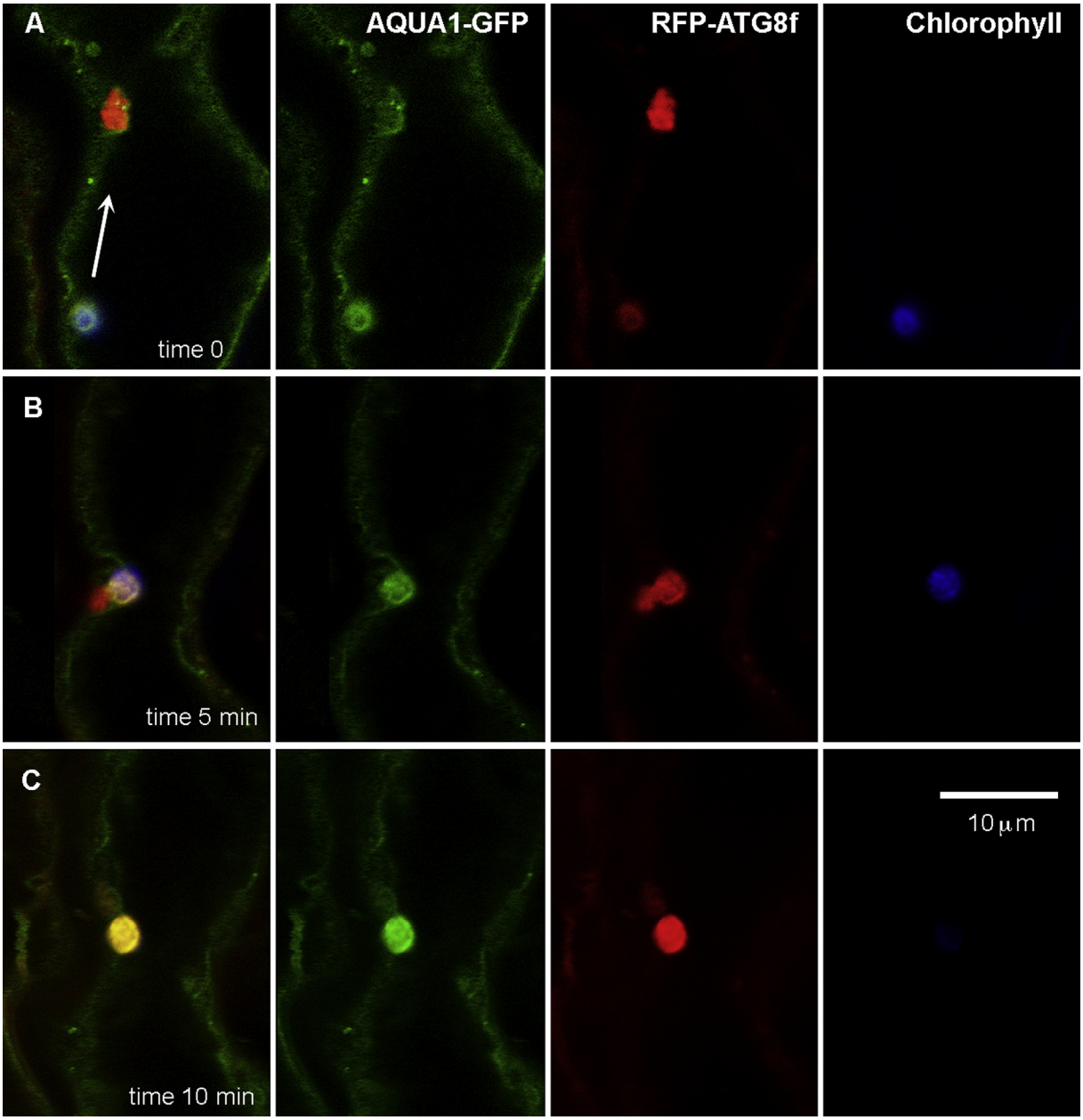

Fig. 3. Imaging of an *Arabidopsis* single epidermal cell co-expression AQUA1-GFP and RFP-ATG8f. A) the AQUA1-GFP fluorescent structure is co-localizing with a chloroplast (blue signal) and moved in the direction indicated by the white arrow, B) after 5 min AQUA1-GFP and RFP-ATG8f labeled structures fused. C) After 5 additional minutes from fusion, the markers where perfectly colocalized and the chlorophyll fluorescence was no more detectable. White arrow indicate the direction of movement. Scale bar 10 µm. (For interpretation of the references to color in this figure legend, the reader is referred to the Web version of this article.)

dispersed and recorded at 500 ÷ 535 nm.

2.10. Image and statistical analysis

Image analysis were performed using Fiji (http://pacific.mpi-cbg.de) and Imaris software (Bitplane, http://www.bitplane.com). To quantify the effects of the different treatments on AQUA1 re-localization the number and total volume of the spots and the vesicles were measured for each cell. ANOVA, post-doc comparison LSD test, Kruskal-Wallis non parametric analysis and regression analysis were using Statistica (StatSoft - http://www.statsoft.it/) and R program (www.r-project.org). Data were normalized if needed.

The comparison of the differences of vesicles number and total volume were performed between different groups: (i) Control and Zn treatment (Zn consider as level), (ii) Zn and Zn + OA (OA consider as level and only Zn as control condition) and (iii) Zn and Zn + Wt (Wt consider as level and only Zn as control condition).

3. Results

3.1. Molecular and expression analysis

The *aqua1*cDNA is a 771bp sequence encoding for a 257 amino acid protein. The nucleotide sequence shows 99% identity with a putative TIP of *Populus trichocarpa* (RefSeqID: XM_002331442.1), with 8 differences in the nucleotide sequence and 2 differences in the amino acid sequence (S3). The gDNA sequence of *aqua1* has shown 2 exons and one intron (S4).

For a deeper understanding of the role of *aqua1* in *Populus x canadensis* I-214 clone in response to excess Zn, a relative quantification by

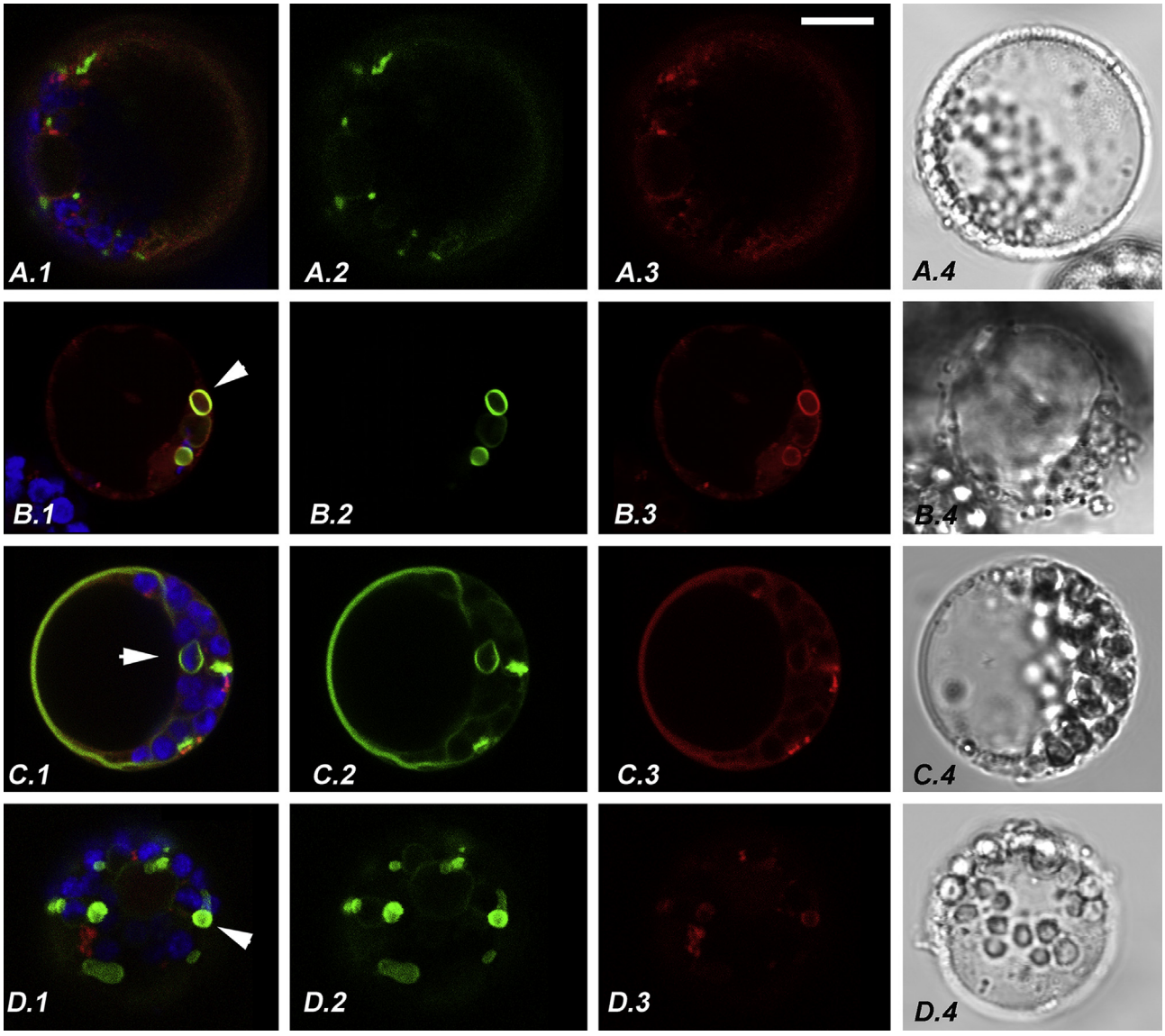

Fig. 4. AQUA1:GFP co-localization in *Arabidopsis* protoplasts. A-B) Co-expressed with Cherry-BP80 labeling ER and small pre-vacuolar compartments (A) as well as larger compartments in stressed cells, as evidenced by the arrow (B) or co-expressed with RFP-ATG8f (D–E) where large compartments become more evident (indicated by arrows) in healthy (C) and stressed cells (D). Column 1 show the merge of all fluorescent emissions: GFP in green, Cherry in red and chlorophyll in blue; column 2 allows to visualize GFP and column 3 Cherry alone. Scale bar 10 μm. (For interpretation of the references to color in this figure legend, the reader is referred to the Web version of this article.)

qPCR was performed in both leaf and root tissues. This analysis confirmed the previous high-throughput results using a microarray on leaf (Di Baccio et al., 2011) and the RNA Sequencing on root (Ariani et al., 2015), showing that *aqua1* was also down-regulated in both tissues in response to excess Zn, with a relative fold change of 0.14 in leaf and 0.06 in root (Fig. 1).

3.2. AQUA1 sub-cellular localization in Arabidopsis

For further characterization of the role of AQUA1 protein, we co-expressed into *Arabidopsis* cotyledon cells two constructs carried in two independent *Agrobacterium* strains. Co-transforming seedlings with 35S:AQUA1-GFP with the plasmatic membrane (PM) marker RFP:AtSYP122, 35S:AQUA1-GFP was clearly localized on internal membranes well different from the plasma membrane (Fig. 2A). Moreover, the aquaporin appeared to have a distribution partially compatible with the ER because it evidenced the nuclear envelope and a peripheric network (Fig. 2A.2). Nonetheless, careful observation revealed that the distribution was not always compatible with ER localization. When co-expressed with the ER marker RFPKDEL (Fig. 2B), it was evident that there was not a perfect co-localization of markers and in some cases, it was clearly visible that the nuclear envelop was not labeled by AQUA1-GFP (Fig. 2B.1 and 2B.2) as it was by RFPKDEL (Fig. 2B.3 red arrow). Also, the well-known fusiform ER-bodies were not completely wrapped by AQUA1-GFP as expected if this protein was on the ER membrane.

AQUA1-GFP labeled membranes did not co-localize with Golgi marker ST-RFP (Fig. 2C) and (even if some patterns could be confused with tonoplast) had a very limited co-localization with the tonoplast marker RFP:AtSYP51 (Fig. 2D). No co-localization was, also, observed when co-expressed with the Pre-Vacuolar Compartment (PVC) marker Cherry-BP80 (Fig. 2E). Despite its distribution clearly distinguished from RFP:AtSYP51, in several cases, AQUA1-GFP appeared to label the tonoplast, as visible in Fig. 2D.

Trying to investigate the relation between AQUA1-GFP distribution, ER and tonoplast, we co-expressed the chimerical construct with the

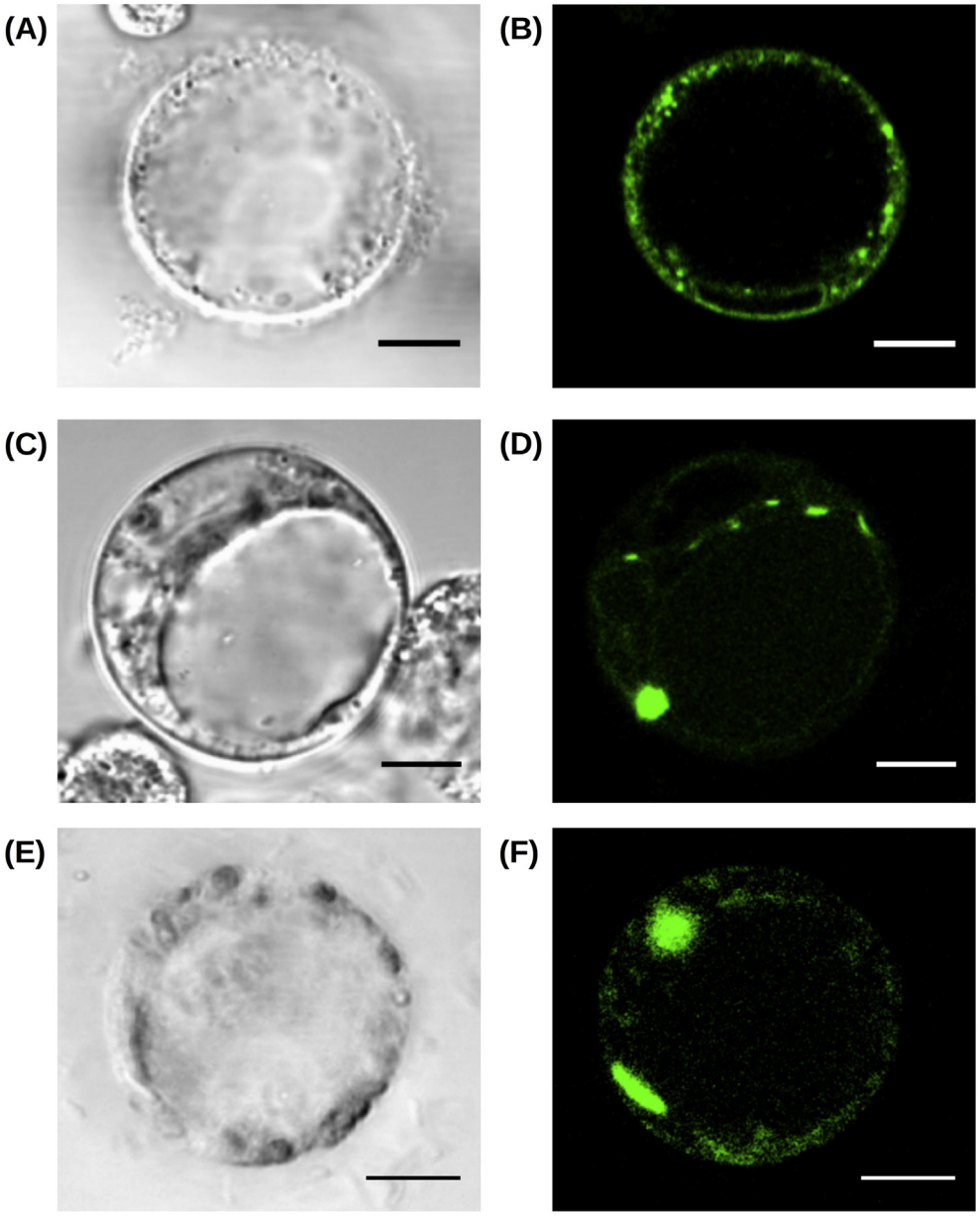

Fig. 5. AQUA1:GFP localization in control and excess Zn conditions. Confocal microscopy images of AQUA1:GFP fusion proteins expressed in *Arabidopsis* protoplast under different Zn concentration. a) Control condition, bright-field; b) Control condition, 488 nm; c) 100 μM Zn, Bright-Field; d) 100 μM Zn, 488 nm; e) 200 μM Zn, bright-field; f) 200 μM Zn, 488 nm. Bars = 10 μm.

autophagosome marker RFP-ATG8f (Fig. 3). This marker is mainly cytosolic but it can form aggregates that should correspond to autophagosomes. No co-localization was observed in small punctate aggregations dispersed in the cytosol, but co-localization was observed in rare large aggregates that occasionally appeared to include chlorophyll fluorescence. In particular, we could image *in vivo* a chloroplast surrounded by AQUA1-GFP fluorescence (Fig. 3A) moving (white arrow indicate the direction of movement) toward a RFP-ATG8f aggregate. In 5 min, the two structure fused (Fig. 3B) and in 5 additional minutes from fusion the chlorophyll fluorescence was completely lost (Fig. 3C).

Fluorescent proteins transiently expressed in differentiated tissue require 48 h to be clearly detectable and in this period their distribution is influenced by several factors. To acquire additional information, the localization of AQUA1-GFP was also studied in *Arabidopsis* (Fig. 4) and *Nicotiana* tabacum (tobacco) (S1 Fig.) protoplasts. In this experimental system markers transient expression is abundant but restricted in time, producing fluorescent pattern often clearer than in intact tissues where expression time is necessarily longer.

We confirmed that AQUA1-GFP does not co-localize with normal distribution of the proposed markers (Fig. 4a) but it can co-localize with Cherry-BP80 (Fig. 4b) and RFP-ATG8f (Fig. 4c-d) in larger Multi-Vesicular Bodies (arrows).

3.3. AQUA1 localization in response to Zn stress

Since *aqua1* was found to be down-regulated in response to Zn stress in leaves and roots, variation of its sub-cellular localization was evaluated in response to Zn stress in transiently transformed protoplast. By adding 100 μM and 200 μM Zn to the protoplast culture media, the localization pattern of AQUA1-GFP was visibly perturbed (Fig. 5d, f). Indeed, there are fewer and larger fluorescent structures in both Zn treatments compared to those observed in the control condition. The reduction in number and the increasing in size were more evident at the highest Zn concentration, where large vesicles appeared (Fig. 5f)

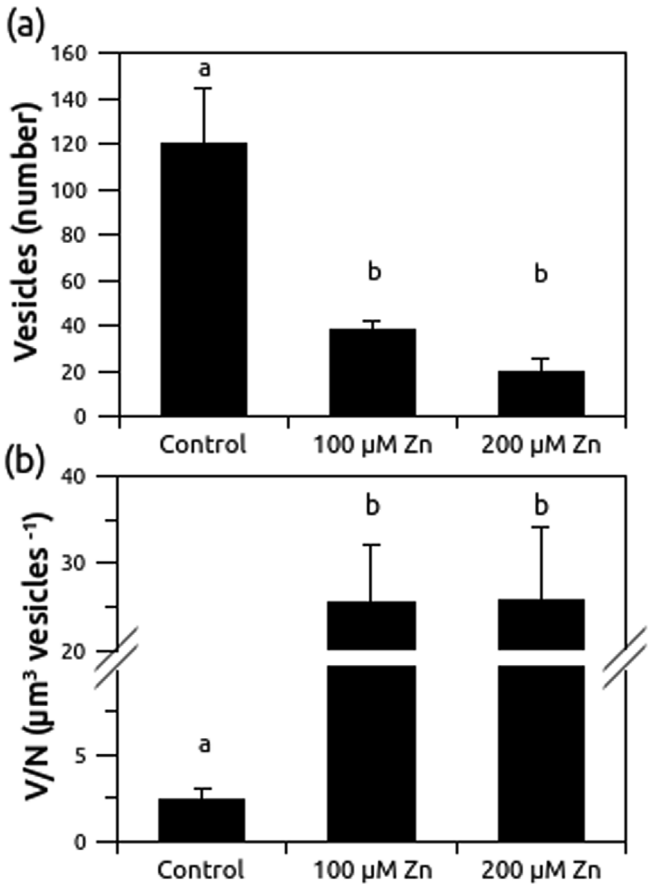

Fig. 6. Vesicles variation in response to Zn in *Arabidopsis* protoplasts. a) Variation of vesicles number in response to different Zn concentration; b) Variation in V/N (volume/number) ratio in response to different Zn concentration. Values represent the averages and the SE of the measurements, different letters within each treatment indicate significant differences at $P < 0.05$ (Kruskal-Wallis test).

coherently with the formation of multivesicular bodies (MVBs).

Statistical analysis showed a significant reduction of vesicles and dispersed structures number ($P < 0.001$), between 3 and 6×, and an increase in the ratio between vesicles total volume and number (V/N) of about 10× ($P < 0.001$) in 100 µM and 200 µM Zn-treated protoplasts. No significant differences were observed across the two Zn treatments (Fig. 6).

3.4. AQUA1 localization in the presence of Hg

Since aquaporin activity is generally inhibited by $HgCl_2$, the sub-cellular localization of AQUA1-GFP was evaluated in transiently transfected *Arabidopsis* protoplast cultured with 10 µM of $HgCl_2$. Confocal microscopy analysis showed that the GFP fluorescent signal disappeared almost completely (Fig. 7b) and very few spots were visible peripherally of the cell. Instead, when the cells were cultured with $HgCl_2$ and 200 µM Zn, the Hg inhibition seemed to be reduced, showing fluorescent spots with a similar visualization pattern as the control (Fig. 7d). Moreover, image analysis confirms this trend, with large vesicle detectable only under $HgCl_2$ and 200 µM Zn treatment (Fig. 7e).

To evaluate if the fluorescence signal of AQUA1-GFP could be restored by DTT, transiently transfected protoplasts were treated for 24 h with $HgCl_2$. After removing Hg and adding DTT, the protoplasts were observed (48 h after initial electroporation). Confocal analysis showed that the sub-cellular localization patterns after the addition of DTT at 24 h from electroporation resemble the ones observed in control condition (S2 Fig.).

3.5. Phosphatases and kinases inhibitors effect on AQUA1 sub-cellular localization

In order to verify if the routing of AQUA1 from spots in the plasmalemma and endomembranes to cytoplasmic vesicles is due to Zn-induced modification of membrane trafficking or AQUA1 activity, we tested the effects of two potent inhibitors of phosphatase (OA) and kinase (Wt), on AQUA1 sub-cellular localization in presence of 200 µM Zn. Wt caused a significant reduction of vesicle numbers between control and drug treatments ($P < 0.05$) of about 50%, with no differences between treatments (Fig. 8), showing a negative correlation of vesicle numbers and increasing Wt concentrations (Pearson' s correlation coefficient = −0.45, $P < 0.05$). Instead there are no significant differences in total vesicles' volume per cell between control and Wt treatments conditions (data not shown).

Moreover, Okadaic acid (OA) caused a significant reduction of vesicle numbers ($P < 0.05$) in the range 0.1–1 µM, but at the higher drug concentration (3 µM) there was no significant difference with control condition (Fig. 9a). Also, total volume was significantly affected by OA ($P < 0.05$), with a significant reduction at the higher drug concentration (3 µM) of about 4× (Fig. 9b). Correlation analysis shows a negative correlation between total vesicle volume and increasing OA concentrations (Spearman' s rank correlation coefficient = −0.36, $P < 0.05$).

3.6. aqua1 confers Zn tolerance in yeast

In order to characterize *aqua1*'s role in mediating Zn response or tolerance, the protein was expressed in yeast BY4741 (wt) and *zrc1/cot1,* a double mutant strain. Heterologous expression of *aqua1* into this mutant complemented *zrc1/cot1* mutations by conferring Zn tolerance up to 100 µM Zn; instead the mutant strain transformed with the empty vector and without the induction of the pYES promoter (-Gal 5%) showed Zn sensitivity at 100 µM Zn (Fig. 10).

4. Discussion

In our previous studies, *aqua1*, an orthologous of *Populus trichocarpa* aquaporin, has been identified as a down-regulated gene in a microarray of leaves and in an RNA sequencing of roots of *P. x canadensis* clone I-214 exposed to excess Zn (Ariani et al., 2015; Di Baccio et al., 2011). The RT-qPCR data confirm this expression pattern in leaves and in roots. Several studies report that aquaporins are differentially expressed in response to metal stress, but the patterns are not uniform and are dependent on the species and type of aquaporins studied (Li et al., 2014). For example, in *Solanum torvum* and *Arabidopsis thaliana* there is a general down regulation of aquaporin transcripts under metal stress (Boursiac et al., 2008; Maathuis et al., 2003; Yamaguchi et al., 2010), while in *Brassica juncea* there is an up regulation of a PIP1 aquaporin that showed improved metal resistance in transgenic over expressing plants (Zhang et al., 2008). In this light, *aqua1* down regulation in both leaf and root tissues of the *P. x canadensis* I-214 clone in response to Zn stress could be a mechanism to reduce transpiration, water/Zn uptake, and leaf growth, probably for protecting photosynthetic tissues and for enhancing poplar tolerance to this stress (Di Baccio et al., 2003; Sebastiani et al., 2004).

The amino acid sequence of AQUA1 contains the typical aquaporins NPA signature motif, which forms the aqueous pore, and have similar responses towards Hg and DTT as other characterized aquaporins (Preston et al., 1993). This suggests that AQUA1 is a Hg-sensitive aquaporin. Indeed, the reduction of fluorescence signal in Hg-treated protoplasts could be interpreted as an enhanced turnover and degradation of the Hg-blocked (non-functional) proteins. In agreement with Preston et al. (1993) and Knipfer et al. (2011), the reversion of normal localization pattern by DTT after Hg treatment confirms this hypothesis.

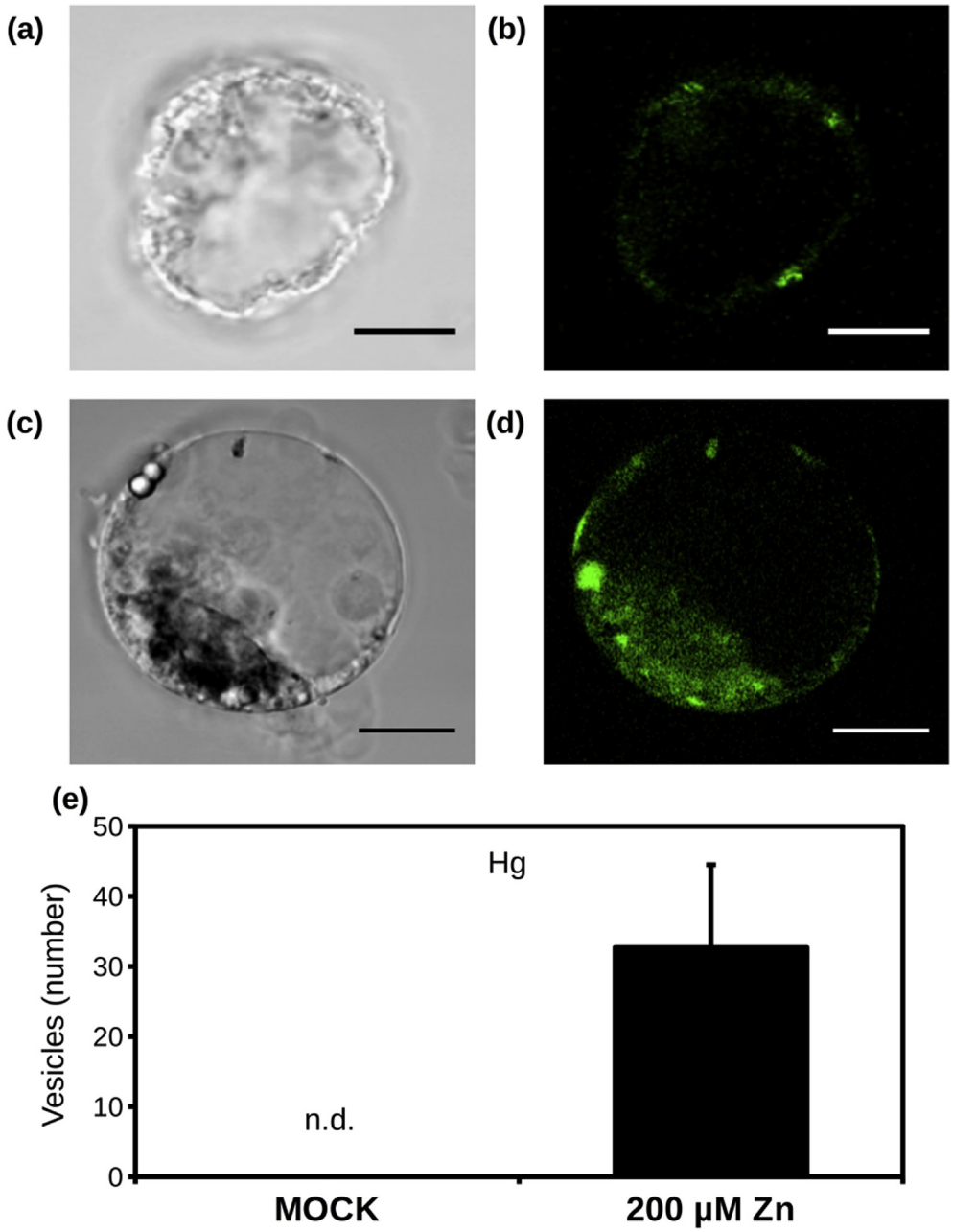

Fig. 7. $HgCl_2$ disrupts AQUA1:GFP fluorescent signal and Zn restores fluorescent signal in the presence of $HgCl_2$. (a–d) Confocal microscopy analysis of AQUA1:GFP fusion proteins expressed in *Arabidopsis* protoplast treated with a) 10 µM $HgCl_2$, brigth-field; b) 10 µM $HgCl_2$, 488 nm; c) 10 µM $HgCl_2$ and 200 µM Zn, bright-field; d) 10 µM $HgCl_2$ and 200 µM Zn, 488 nm. Bars = 10 µM. e) Variation in vesicles number in response to 0 (Control) and 200 µM Zn with a constant 10 µM concentration of $HgCl_2$. Values represent the averages and the SD of the measurements.

In the last years, several aquaporins with *non-aqua* functions have been identified and characterized (Hove and Bhave, 2011). These aquaporins can transport ammonia, hydrogen peroxide, carbon dioxide and also metals. Since over expression of *aqua1* in transgenic *Populus* plants did not increase Zn accumulation under excess Zn conditions (Ariani et al., 2016), the ability of *aqua1* to complement the phenotype of the Zn hypersensitive *zrc1/cot1* mutant yeast strain could be interpreted as a protective effect of this gene aimed at regulating water potential in response to metal stress or at increasing cellular growth. This hypothesis is supported by the overexpression of the barley aquaporin *HvPIP2;*5 that confers salt and osmotic stress tolerance in yeast and plants (Alavilli et al., 2016).

The localization of the GFP-tagged protein indicated a diffused distribution (often observed for several over expressed aquaporins) but specifically leading to MVBs co-localization together with other markers typical of PVC and autophagosomes.

The true identity of the observed multivesicular bodies (MVBs) cannot be stated. The MVBs formation and function is far from being fully elucidated. It is reasonable to speculate they may become specialized vacuoles when heterotypic fusion is impaired. Other membranous structures have been described such as dark-induced protein (DIP) vesicles characterized by the presence of aquaporins and RMR-like proteins (Jiang et al., 2001). DIP vesicles are the main system for transporting crystalloid elements to the protein storage vacuoles (PSVs) (Vitale and Hinz, 2005) and are surrounded by a double membrane that fuses with PSVs, delivering the inner membrane that forms an independent compartment inside PSVs (Isaienkov, 2014). Also, autophagosomes have a double membrane and are capable to fuse with the

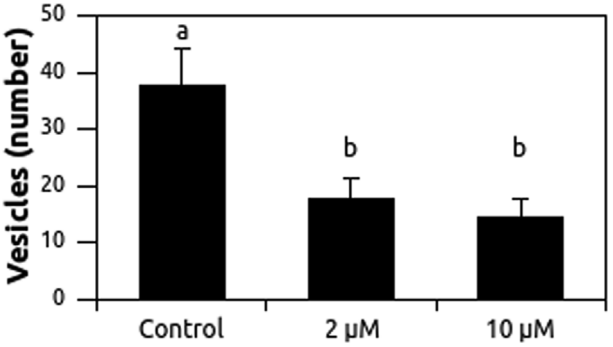

Fig. 8. Wortmannin (Wt) reduces the number of AQUA1 cytosolic vesicles in response to excess Zn. Comparison of the variations in vesicles' number in response to 0 (Control), 2 and 10 µM Wt with a constant 200 µM concentration of Zn. Values represent the averages and the SE of the measurements, different letters within each treatment indicate significant differences at $P < 0.05$ (Kruskal-Wallis test).

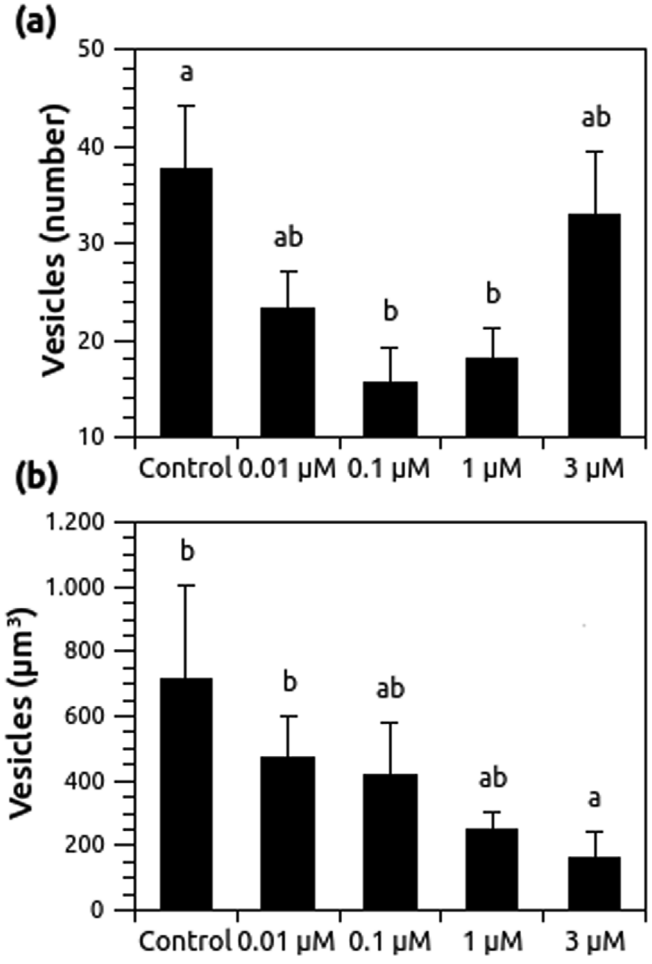

Fig. 9. Okadaic acid (OA) affects both vesicles number and total volume of AQUA1 cytosolic vesicles in response to excess Zn. a) Variation of vesicles number in response to different OA concentration and a constant 200 µM concentration of Zn. Different letters within each treatment indicate significant differences at $P < 0.05$ (Kruskal-Wallis test); b) Variation of vesicles volume in response to different OA concentration and a constant 200 µM concentration of Zn, the data has been normalized as $1/\log_n$. Different letters indicate significant differences at $P < 0.05$ (LSD test with false discovery rate correction). Values represent the averages and the SE of the measurements.

vacuole (Bassham and Crespo, 2014). The imaging presented here did not allow to appreciate how AQUA1-related MVBs had double membrane, but it was clearly confirmed by imaging in tobacco. AQUA1-related MVBs may influence vacuolar homeostasis directly, changing its composition, or indirectly, producing autonomous compartments for homeostasis.

The reduction of Hg inhibition of AQUA1 in the presence of 200 µM of Zn, with its localization pattern similar to control condition, and the significant increase in vesicle number in *Arabidopsis* protoplasts under excess Zn, suggest a direct relationship between Zn and AQUA1 localization, highlighting a protective role of this protein.

The best blast hit of *aqua1* is a *Populus trichocarpa* aquaporin that belong to the TIP sub-family, a class of aquaporins which usually localize in the tonoplast of plant cells and have been widely used as vacuolar markers in several studies (reviewed in Frigerio et al., 2008; Gattolin et al., 2010). However, aquaporins co-localization may be confusing, as confirmed by Gattolin et al. (2011) reporting *Arabidopsis* TIPs localization in both the plasmalemma and tonoplast during seed maturation and germination, thus reflecting a more complex and fine-tuned regulation of TIP aquaporins in different physiological contexts.

Zn treatments caused the re-localization of AQUA1 only in aggregated structures, with no fluorescent signal associated to the ER. The significant reduction in number, together with the increase in the volume/number (V/N) ratio, could suggests AQUA1-related MVBs' aggregation in response to Zn stress. The formation of these compartments may remove aquaporins from the ER reducing its permeability or concentrate all the activity in the new compartment. A similar mechanism of re-localization has been reported for the human aquaporin-2 in response to hormone-signaling in the renal collecting duct (Moeller and Fenton, 2012) and for *Arabidopsis* PIPs in root subjected to NaCl and salicylic acid treatments (Boursiac et al., 2008), accompanied with the re-localization of AtTIP1 in small double-membrane vacuolar invaginations called 'bulbs'. In fact, AQUA1-GFP co-localized with *Arabidopsis* vacuolar marker AtTIP1;1 (not shown).

The formation of separated vacuoles is a general mechanism to counteract metal stress in both plant and animals, and previous studies report that in *Arabidopsis* cells Zn detoxification was mainly mediated by specific vacuolar metal transporter such as AtMTP1 and AtHMA3 (Desbrosses-Fonrouge et al., 2005; Morel et al., 2009). AtMTP1 localizes mainly at vacuolar level, and *mtp1* mutants did not form Zn-accumulating vesicles when exposed to excess Zn (Kawachi et al., 2009), suggesting an additional role for this protein in such Zn-induced vesicles. These Zn-accumulating vesicles have been previously identified in yeast and mammalian cells (Devirgiliis et al., 2004; Eide, 2006; Haase and Beyersmann, 2002) and are designated as 'zincosomes'.

It is likely that the previously found vesicles (Kawachi et al., 2009) have similar function to those observed in our experiments. Indeed, AQUA1 could be involved in Zn storage in these new compartments by regulating water flow across their membranes and buffering osmotic potential within the cytosol. The aquaporin internalization has been previously observed by Ueda et al. (2016) which report that AtPIP2;1 is constitutively trafficked between the PM and the trans-Golgi network (TGN) in *Arabidopsis thaliana*. Under salt stress condition PIP2;1 relocalizes into intracellular compartments to decrease the water permeability. The same behavior has been also confirmed by Chu et al. (2018) which observed a specific relocalization of plasma membrane aquaporins into intracellular compartments depending on the isoform, the cell type or the treatment.

Investigating aquaporins endocytosis is generally interesting because it reduces plasma membrane permeability. In this case, AQUA1 was not observed in the plasma membrane. Anyhow the unclear distribution of AQUA1 in endomembranes required further investigations to understand if trafficking occurred through the classic Golgi-dependent vacuolar sorting path or other emerging pathways (Occhialini et al., 2016) bypassing the Golgi. Stress-dependent endocytosis of aquaporins could be regulated by two different mechanisms which involve protein kinases: the first is mediated by phosphatidylinositol 3-kinase (PI3K) activity, which modulates the intracellular membrane

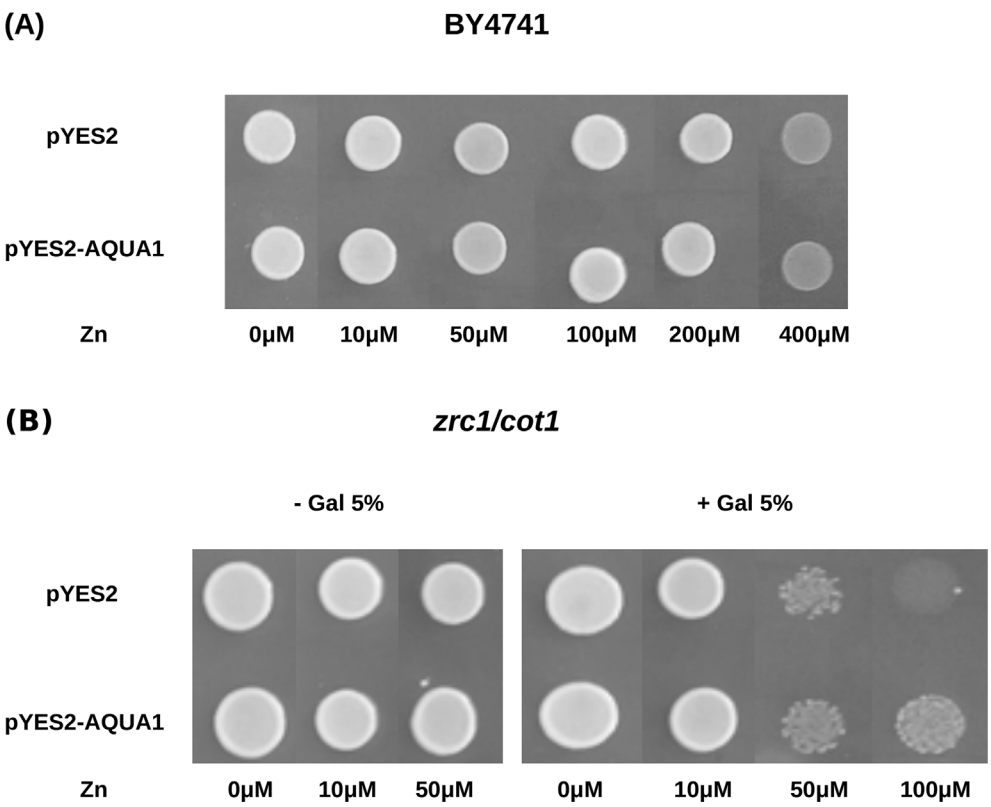

Fig. 10. AQUA1 confers Zn tolerance when expressed in yeast. Complementation experiment of *aqua1* in yeast. a) Control transformation of wild type strain (BY4741) with the empty vector (pYES2) and with the vector containing the coding sequence of *aqua1* (pYES-AQUA1) cultured under different Zn concentration in the growth media b) Transformation of *zrt1/cot1* mutant strain with the empty vector (pYES2) and with the vector containing the coding sequence of *aqua1* (pYES-AQUA1), cultured under different Zn concentration and the presence (+Gal 5%) or absence (- Gal 5%) of galactose in the growth media.

trafficking by regulating phosphatidylinositol 3-P availability (Santiago-Tirado and Bretscher, 2011; Simonsen et al., 2001); the second involves multiple phosphorylation in the C-terminus of aquaporins (Boursiac et al., 2008; Prak et al., 2008). *Arabidopsis* mutant for PI3K and *wt* plants treated with wortmannin (a specific inhibitor of PI3K) showed suppression of endocytosis in response to salt stress, which could be rescued by supplementation with exogenous phosphatidylinositol 3-P. Studies using the toxin wortmannin showed that also the vacuoles heterologous fusion, and consequently vacuolar sorting, depends on PI3K (Di Sansebastiano et al., 2007; Jiang and Rogers, 1998; Zheng et al., 2014a, 2014b).

The significant reduction in vesicle numbers, together with the negative correlation of AQUA1-GFP-labeled MVBs in *Arabidopsis* protoplast, treated with 200 μM Zn and wortmannin, could suggest a PI3K-mediated endocytosis of AQUA1 or a reduction in MVBs formation under Zn stress. Since wortmannin could inhibit also other kinases (Liu et al., 2007, 2005), it is not possible to discriminate between the effect of traffic and of the re-localization mediated by phosphorylation in the C-terminus of AQUA1 in response to Zn stress. This regulation could be achieved by phosphorylation of AQUA1 in order to modulate the gating of this channel, and phosphatases inhibitors, like OA acid, could disrupt this process. OA blocks aquaporins in an open conformation by interfering with the phosphorylation state of specific residues in the N− and C-terminus of the protein (Chaumont et al., 2005; Horie et al., 2011; Prak et al., 2008). *Xenopus* oocyte overexpressing PIP2;1 aquaporin of *Mesembryanthemum crystallinum* showed modifications of the relative volume increase, osmotic water permeability and protein phosphorylation level under OA treatments (Amezcua-Romero et al., 2010), highlighting the importance of post-translational modifications in the regulation of aquaporins' activity. The variation in MVBs' volume observed in protoplasts treated with OA, with the significant reduction at the higher OA concentration (3 μM) and a significant negative correlation, could suggests that AQUA1 phosphorylation regulates the activity of this protein in response to excess Zn. The open-blocked conformation of AQUA1 could reduce vesicles' volumes, since they are unable to control water flow across their membranes. This impairment could be buffered by an increase in vesicle aggregation, as suggested by the reduction of vesicles' number in the range 0.1–1 μM of OA concentration. At 3 μM of OA the vesicle number was not significantly different from control condition. This could be explained by a cytotoxic effect of this OA concentration that inhibits microtubule organization (Perreault et al., 2012; Sheremet et al., 2009), and probably blocks vesicles' aggregation and intracellular trafficking in our experimental system.

5. Conclusions

A number of papers have clearly demonstrated the aquaporin involvement in abiotic stress, thus suggesting that, as in soybean, the over expression may increase stress tolerance (Lu et al., 2018). On the contrary, the aquaporin functional mechanism is not fully characterized, maybe due to many isoforms and cell types. However, all data seem to confirm that aquaporins are involved in water homeostasis in cell at all phylogenetic levels of life, due to their ability to relocalize. Indeed, the phosphorylation was found to play a central role in the mechanisms that determine their gating and subcellular dynamics (Jang et al., 2014; Kitchen et al., 2015; Verdoucq et al., 2014).

In conclusion, in agreement with the above scenario, we demonstrated that AQUA1 is a Hg-sensitive aquaporin regulated both at transcriptional and post-translational levels in response to Zn stress. Indeed, Zn determines the relocalization of AQUA1 in new forming compartments by affecting both AQUA1 intracellular trafficking and activity. The down regulation in both leaves and roots of *P. x canadensis* I-214 clone in response to Zn stress could be explained as a defense mechanism for reducing water flow and plants growth in response to this stress. Moreover, AQUA1 re-localization and post-translational modification observed in *Arabidopsis* protoplasts could be involved in reducing water flow and adjusting cellular osmotic potential in response to Zn excess.

Funding

This work was supported by a grant from the “Cassa di Risparmio di San Miniato” Foundation (ID: 2008.0361). Special thanks to the “Regione Puglia” for supporting the Project no. 14 “Reti di Laboratori Pubblici di Ricerca” “SELGE”. Andrea Ariani scholarship was granted by Agrobioscience PhD program at Scuola Superiore Sant’Anna of Pisa (ID: PAGR26).

Author contribution

All the Authors have contributed equally to the manuscript. In particular, Andrea Ariani made most of the experiments, the statistical analysis and contributed to write the paper. Fabio Barzotti and Gian Pietro di San Sebastiano made the Arabidopsis plant and tobacco transfections and the relative confocal observations and contributed to write the paper. Luca Sebastiani made the statistical analysis, contributed to the experimental design and to write the paper. Luigi Sanità di Toppi contributed to the experimental design and to write the paper. Andrea Andreucci made some experiments, most of the confocal observations on Arabidopsis protoplasts, contributed to the experimental design and to write the paper.

Acknowledgements

The authors would like to thank Antonio Masini for his technical support. We wish to thank Prof. Ute Krämer (Max Planck Institute of Molecular Plant Physiology, Potsdam, Germany) for providing us with yeast strains. Also, special thanks to Dr Cristina Di Primio for technical assistance with the confocal microscope and to “SELGE - Regione Puglia, Reti di Laboratori Pubblici di Ricerca” for confocal microscope imaging of co-localizations.

Appendix A. Supplementary data

Supplementary data to this article can be found online at https://doi.org/10.1016/j.plaphy.2018.10.038.

References

Alavilli, H., Awasthi, J.P., Rout, G.R., Sahoo, L., Lee, B.-H., Panda, S.K., 2016. Overexpression of a barley aquaporin gene, HvPIP2;5 confers salt and osmotic stress tolerance in yeast and plants. Front. Plant Sci. 7, 1566.

Amezcua-Romero, J.C., Pantoja, O., Vera-Estrella, R., 2010. Ser123 is essential for the water channel activity of McPIP2;1 from *Mesembryanthemum crystallinum*. J. Biol. Chem. 285, 16739–16747.

Ariani, A., Di Baccio, D., Romeo, S., Lombardi, L., Andreucci, A., Lux, A., Horner, D.S., Sebastiani, L., 2015. RNA sequencing of *Populus x canadensis roots* identifies key molecular mechanisms underlying physiological adaption to excess zinc. PloS One 10, e0117571.

Ariani, A., Francini, A., Andreucci, A., Sebastiani, L., 2016. Over-expression of AQUA1 in *Populus alba* Villafranca clone increases relative growth rate and water use efficiency, under Zn excess condition. Plant Cell Rep. 35, 289–301.

Di Baccio, D., Minnocci, A., Sebastiani, L., 2010. Leaf structural modifications in Populus × euramericana subjected to Zn excess. Biol. Plant. 54, 502–508.

Di Baccio, D., Tognetti, R., Sebastiani, L., Vitagliano, C., 2003. Responses of Populus deltoides × Populus nigra (Populus × euramericana) clone I-214 to high zinc concentrations. New Phytol. 159, 443–452.

Bassham, D.C., Crespo, J.L., 2014. Autophagy in plants and algae. Front. Plant Sci. 5, 679.

Boursiac, Y., Prak, S., Boudet, J., Postaire, O., Luu, D.-T., Tournaire-Roux, C., Santoni, V., Maurel, C., 2008. The response of Arabidopsis root water transport to a challenging environment implicates reactive oxygen species- and phosphorylation-dependent internalization of aquaporins. Plant Signal. Behav. 3, 1096–1098.

Broadley, M.R., White, P.J., Hammond, J.P., Zelko, I., Lux, A., 2007. Zinc in plants. New Phytol. 173, 677–702.

Brunner, A.M., Yakovlev, I.A., Strauss, S.H., 2004. Validating internal controls for quantitative plant gene expression studies. BMC Plant Biol. 4, 14.

Castiglione, S., Todeschini, V., Franchin, C., Torrigiani, P., Gastaldi, D., Cicatelli, A., Rinaudo, C., Berta, G., Biondi, S., Lingua, G., 2009. Clonal differences in survival capacity, copper and zinc accumulation, and correlation with leaf polyamine levels in poplar: a large-scale field trial on heavily polluted soil. Environ. Pollut. 157, 2108–2117.

Chaumont, F., Barrieu, F., Wojcik, E., Chrispeels, M.J., Jung, R., 2001. Aquaporins constitute a large and highly divergent protein family in maize. Plant Physiol. 125, 1206–1215.

Chaumont, F., Moshelion, M., Daniels, M.J., 2005. Regulation of plant aquaporin activity. Biol. Cell 97, 749–764.

Chevalier, A.S., Chaumont, F., 2015. Trafficking of plant plasma membrane aquaporins: multiple regulation levels and complex sorting signals. Plant Cell Physiol. 56, 819–829.

Chu, T.T.H., Hoang, T.G., Trinh, D.C., Bureau, C., Meynard, D., Vernet, A., Ingouff, M., Do, N.V., Périn, C., Guiderdoni, E., Gantet, P., Maurel, C., Luu, D.-T., 2018. Subcellular markers highlight intracellular dynamics of membrane proteins in response to abiotic treatments in rice. Rice (N Y) 11.

Danielson, J.A.H., Johanson, U., 2008. Unexpected complexity of the aquaporin gene family in the moss *Physcomitrella patens*. BMC Plant Biol. 8, 45.

De Benedictis, M., Bleve, G., Faraco, M., Stigliano, E., Grieco, F., Piro, G., Dalessandro, G., Di Sansebastiano, G.P., 2013. AtSYP51/52 functions diverge in the post-Golgi traffic and differently affect vacuolar sorting. Mol. Plant 6, 916–930.

Desbrosses-Fonrouge, A.-G., Voigt, K., Schröder, A., Arrivault, S., Thomine, S., Krämer, U., 2005. *Arabidopsis thaliana* MTP1 is a Zn transporter in the vacuolar membrane which mediates Zn detoxification and drives leaf Zn accumulation. FEBS Lett. 579, 4165–4174.

Devirgiliis, C., Murgia, C., Danscher, G., Perozzi, G., 2004. Exchangeable zinc ions transiently accumulate in a vesicular compartment in the yeast *Saccharomyces cerevisiae*. Biochem. Biophys. Res. Commun. 323, 58–64.

Di Baccio, D., Galla, G., Bracci, T., Andreucci, A., Barcaccia, G., Tognetti, R., Sebastiani, L., 2011. Transcriptome analyses of *Populus x euramericana* clone I-214 leaves exposed to excess zinc. Tree Physiol. 31, 1293–1308.

Di Baccio, D., Tognetti, R., Minnocci, A., Sebastiani, L., 2009. Responses of the *Populus*×*euramericana* clone I-214 to excess zinc: carbon assimilation, structural modifications, metal distribution and cellular localization. Environ. Exp. Bot. 67, 153–163.

Di Sansebastiano, G.P., Rehman, R.U., Neuhaus, J.-M., 2007. Rat β-glucuronidase as a reporter protein for the analysis of the plant secretory pathway. Plant Biosyst. Int. J. Deal. Aspect Plant Biol. 141, 329–336.

Dos Santos Utmazian, M.N., Wieshammer, G., Vega, R., Wenzel, W.W., 2007. Hydroponic screening for metal resistance and accumulation of cadmium and zinc in twenty clones of willows and poplars. Environ. Pollut. 148, 155–165.

Eide, D.J., 2006. Zinc transporters and the cellular trafficking of zinc. Biochim. Biophys. Acta 1763, 711–722.

Frigerio, L., Hinz, G., Robinson, D.G., 2008. Multiple vacuoles in plant cells: rule or exception? Traffic 9, 1564–1570.

Gattolin, S., Sorieul, M., Frigerio, L., 2011. Mapping of tonoplast intrinsic proteins in maturing and germinating Arabidopsis seeds reveals dual localization of embryonic TIPs to the tonoplast and plasma membrane. Mol. Plant 4, 180–189.

Gattolin, S., Sorieul, M., Frigerio, L., 2010. Tonoplast intrinsic proteins and vacuolar identity. Biochem. Soc. Trans. 38, 769–773.

Gerbeau, P., Amodeo, G., Henzler, T., Santoni, V., Ripoche, P., Maurel, C., 2002. The water permeability of Arabidopsis plasma membrane is regulated by divalent cations and pH. Plant J. 30, 71–81.

Gietz, R.D., Schiestl, R.H., Willems, A.R., Woods, R.A., 1995. Studies on the transformation of intact yeast cells by the LiAc/SS-DNA/PEG procedure. Yeast 11, 355–360.

Gomes, D., Agasse, A., Thiébaud, P., Delrot, S., Gerós, H., Chaumont, F., 2009. Aquaporins are multifunctional water and solute transporters highly divergent in living organisms. Biochim. Biophys. Acta 1788, 1213–1228.

Gupta, A.B., Sankararamakrishnan, R., 2009. Genome-wide analysis of major intrinsic proteins in the tree plant *Populus trichocarpa*: characterization of XIP subfamily of aquaporins from evolutionary perspective. BMC Plant Biol. 9, 134.

Haase, H., Beyersmann, D., 2002. Intracellular zinc distribution and transport in C6 rat glioma cells. Biochem. Biophys. Res. Commun. 296, 923–928.

Hachez, C., Laloux, T., Reinhardt, H., Cavez, D., Degand, H., Grefen, C., De Rycke, R., Inzé, D., Blatt, M.R., Russinova, E., Chaumont, F., 2014a. Arabidopsis SNAREs SYP61 and SYP121 coordinate the trafficking of plasma membrane aquaporin PIP2;7 to modulate the cell membrane water permeability. Plant Cell 26, 3132–3147.

Hachez, C., Veljanovski, V., Reinhardt, H., Guillaumot, D., Vanhee, C., Chaumont, F., Batoko, H., 2014b. The Arabidopsis abiotic stress-induced TSPO-related protein reduces cell-surface expression of the aquaporin PIP2;7 through protein-protein interactions and autophagic degradation. Plant Cell 26, 4974–4990.

Hirano, Y., Okimoto, N., Kadohira, I., Suematsu, M., Yasuoka, K., Yasui, M., 2010. Molecular mechanisms of how mercury inhibits water permeation through aquaporin-1: understanding by molecular dynamics simulation. Biophys. J. 98, 1512–1519.

Horie, T., Kaneko, T., Sugimoto, G., Sasano, S., Panda, S.K., Shibasaka, M., Katsuhara, M., 2011. Mechanisms of water transport mediated by PIP aquaporins and their regulation via phosphorylation events under salinity stress in barley roots. Plant Cell Physiol. 52, 663–675.

Hove, R.M., Bhave, M., 2011. Plant aquaporins with non-aqua functions: deciphering the signature sequences. Plant Mol. Biol. 75, 413–430.

Isaienkov, S.V., 2014. Plant vacuoles: physiological roles and mechanisms of vacuolar sorting and vesicular trafficking. Tsitol. Genet. 48, 71–82.

Jang, H.-Y., Rhee, J., Carlson, J.E., Ahn, S.-J., 2014. The Camelina aquaporin CsPIP2;1 is regulated by phosphorylation at Ser273, but not at Ser277, of the C-terminus and is involved in salt- and drought-stress responses. J. Plant Physiol. 171, 1401–1412.

Javot, H., Maurel, C., 2002. The role of aquaporins in root water uptake. Ann. Bot. 90, 301–313.

Jiang, L., Phillips, T.E., Hamm, C.A., Drozdowicz, Y.M., Rea, P.A., Maeshima, M., Rogers, S.W., Rogers, J.C., 2001. The protein storage vacuole: a unique compound organelle. J. Cell Biol. 155, 991–1002.

Jiang, L., Rogers, J.C., 1998. Integral membrane protein sorting to vacuoles in plant cells: evidence for two pathways. J. Cell Biol. 143, 1183–1199.

Johanson, U., Karlsson, M., Johansson, I., Gustavsson, S., Sjövall, S., Fraysse, L., Weig, A.R., Kjellbom, P., 2001. The complete set of genes encoding major intrinsic proteins in Arabidopsis provides a framework for a new nomenclature for major intrinsic proteins in plants. Plant Physiol. 126, 1358–1369.

Kawachi, M., Kobae, Y., Mori, H., Tomioka, R., Lee, Y., Maeshima, M., 2009. A mutant strain *Arabidopsis thaliana* that lacks vacuolar membrane zinc transporter MTP1 revealed the latent tolerance to excessive zinc. Plant Cell Physiol. 50, 1156–1170.
Kitchen, P., Day, R.E., Taylor, L.H.J., Salman, M.M., Bill, R.M., Conner, M.T., Conner, A.C., 2015. Identification and molecular mechanisms of the rapid tonicity-induced relocalization of the aquaporin 4 channel. J. Biol. Chem. 290, 16873–16881.
Knipfer, T., Besse, M., Verdeil, J.-L., Fricke, W., 2011. Aquaporin-facilitated water uptake in barley (*Hordeum vulgare* L.) roots. J. Exp. Bot. 62, 4115–4126.
Kuzovkina, Y.A., Quigley, M.F., 2005. Willows beyond wetlands: uses of *Salix* L. Species for environmental projects. Water Air Soil Pollut. 162, 183–204.
Lado, L.R., Hengl, T., Reuter, H.I., 2008. Heavy metals in European soils: a geostatistical analysis of the FOREGS Geochemical database. Geoderma 148, 189–199.
Laureysens, I., De Temmerman, L., Hastir, T., Van Gysel, M., Ceulemans, R., 2005. Clonal variation in heavy metal accumulation and biomass production in a poplar coppice culture. II. Vertical distribution and phytoextraction potential. Environ. Pollut. 133, 541–551.
Lee, H.K., Cho, S.K., Son, O., Xu, Z., Hwang, I., Kim, W.T., 2009. Drought stress-induced Rma1H1, a RING membrane-anchor E3 ubiquitin ligase homolog, regulates aquaporin levels via ubiquitination in transgenic Arabidopsis plants. Plant Cell 21, 622.
Li, G., Santoni, V., Maurel, C., 2014. Plant aquaporins: roles in plant physiology. Biochim. Biophys. Acta 1840, 1574–1582.
Li, J.-F., Park, E., von Arnim, A.G., Nebenführ, A., 2009. The FAST technique: a simplified Agrobacterium-based transformation method for transient gene expression analysis in seedlings of Arabidopsis and other plant species. Plant Methods 5, 6.
Li, X., Poon, C., Liu, P.S., 2001. Heavy metal contamination of urban soils and street dusts in Hong Kong. Appl. Geochem. 16, 1361–1368.
Li, X., Zhang, X., Wu, Y., Li, B., Yang, Y., 2018. Physiological and biochemical analysis of mechanisms underlying cadmium tolerance and accumulation in turnip. Plant Divers. 40, 19–27.
Liu, Y., Jiang, N., Wu, J., Dai, W., Rosenblum, J.S., 2007. Polo-like kinases inhibited by wortmannin. Labeling site and downstream effects. J. Biol. Chem. 282, 2505–2511.
Liu, Y., Shreder, K.R., Gai, W., Corral, S., Ferris, D.K., Rosenblum, J.S., 2005. Wortmannin, a widely used phosphoinositide 3-kinase inhibitor, also potently inhibits mammalian polo-like kinase. Chem. Biol. 12, 99–107.
Livak, K.J., Schmittgen, T.D., 2001. Analysis of relative gene expression data using real-time quantitative PCR and the 2(-Delta Delta C(T)) Method. Methods 25, 402–408.
Lu, L., Dong, C., Liu, R., Zhou, B., Wang, C., Shou, H., 2018. Roles of soybean plasma membrane intrinsic protein GmPIP2;9 in drought tolerance and seed development. Front. Plant Sci. 9, 530.
Maathuis, F.J.M., Filatov, V., Herzyk, P., Krijger, G.C., Axelsen, K.B., Chen, S., Green, B.J., Li, Y., Madagan, K.L., Sánchez-Fernández, R., Forde, B.G., Palmgren, M.G., Rea, P.A., Williams, L.E., Sanders, D., Amtmann, A., 2003. Transcriptome analysis of root transporters reveals participation of multiple gene families in the response to cation stress. Plant J. 35, 675–692.
MacDiarmid, C.W., Milanick, M.A., Eide, D.J., 2003. Induction of the ZRC1 metal tolerance gene in zinc-limited yeast confers resistance to zinc shock. J. Biol. Chem. 278, 15065–15072.
Maurel, C., Verdoucq, L., Luu, D.-T., Santoni, V., 2008. Plant aquaporins: membrane channels with multiple integrated functions. Annu. Rev. Plant Biol. 59, 595–624.
Mertens, J., Vervaeke, P., Meers, E., Tack, F.M.G., 2006. Seasonal changes of metals in willow (*Salix* sp.) stands for phytoremediation on dredged sediment. Environ. Sci. Technol. 40, 1962–1968.
Michaeli, S., Honig, A., Levanony, H., Peled-Zehavi, H., Galili, G., 2014. Arabidopsis ATG8-INTERACTING PROTEIN1 is involved in autophagy-dependent vesicular trafficking of plastid proteins to the vacuole. Plant Cell 26, 4084–4101.
Moeller, H.B., Fenton, R.A., 2012. Cell biology of vasopressin-regulated aquaporin-2 trafficking. Pflügers Archiv 464, 133–144.
Morel, M., Crouzet, J., Gravot, A., Auroy, P., Leonhardt, N., Vavasseur, A., Richaud, P., 2009. AtHMA3, a P1B-ATPase allowing Cd/Zn/Co/Pb vacuolar storage in Arabidopsis. Plant Physiol. 149, 894–904.
Nesler, A., DalCorso, G., Fasani, E., Manara, A., Di Sansebastiano, G.P., Argese, E., Furini, A., 2017. Functional components of the bacterial CzcCBA efflux system reduce cadmium uptake and accumulation in transgenic tobacco plants. Nat. Biotechnol. 35, 54–61.
Occhialini, A., Gouzerh, G., Di Sansebastiano, G.-P., Neuhaus, J.-M., 2016. Dimerization of the vacuolar receptors AtRMR1 and -2 from *Arabidopsis thaliana* contributes to their localization in the trans-golgi network. Int. J. Mol. Sci. 17.
Perreault, F., Matias, M.S., Oukarroum, A., Matias, W.G., Popovic, R., 2012. Okadaic acid inhibits cell growth and photosynthetic electron transport in the alga *Dunaliella tertiolecta*. Sci. Total Environ. 414, 198–204.
Pitto, L., Cernilogar, F., Evangelista, M., Lombardi, L., Miarelli, C., Rocchi, P., 2000. Characterization of carrot nuclear proteins that exhibit specific binding affinity towards conventional and non-conventional DNA methylation. Plant Mol. Biol. 44, 659–673.
Prak, S., Hem, S., Boudet, J., Viennois, G., Sommerer, N., Rossignol, M., Maurel, C., Santoni, V., 2008. Multiple phosphorylations in the C-terminal tail of plant plasma membrane aquaporins: role in subcellular trafficking of AtPIP2;1 in response to salt stress. Mol. Cell. Proteomics 7, 1019–1030.
Preston, G.M., Jung, J.S., Guggino, W.B., Agre, P., 1993. The mercury-sensitive residue at cysteine 189 in the CHIP28 water channel. J. Biol. Chem. 268, 17–20.
Pulford, I.D., Dickinson, N., 2005. Phytoremediation technologies using trees. In: Trace Elements in the Environment.
Pulford, I.D., Watson, C., Mcgregor, S.D., 2001. Uptake of chromium by trees: prospects for phytoremediation. Environ. Geochem. Health 23, 307–311.
Quigley, F., Rosenberg, J.M., Shachar-Hill, Y., Bohnert, H.J., 2002. From genome to function: the Arabidopsis aquaporins. Genome Biol. 3.
Rehman, R.U., Stigliano, E., Lycett, G.W., Sticher, L., Sbano, F., Faraco, M., Dalessandro, G., Di Sansebastiano, G.-P., 2008. Tomato Rab11a characterization evidenced a difference between SYP121-dependent and SYP122-dependent exocytosis. Plant Cell Physiol. 49, 751–766.
Rigola, D., Fiers, M., Vurro, E., Aarts, M.G.M., 2006. The heavy metal hyperaccumulator *Thlaspi caerulescens* expresses many species-specific genes, as identified by comparative expressed sequence tag analysis. New Phytol. 170, 753–765.
Saint-Jore-Dupas, C., Nebenfuhr, A., Boulaflous, A., Follet-Gueye, M.L., Plasson, C., Hawes, C., Driouich, A., Faye, L., Gomord, V., 2006. Plant N-glycan processing enzymes employ different targeting mechanisms for their spatial arrangement along the secretory pathway. Plant Cell 18, 3182–3200.
Sakurai, J., Ishikawa, F., Yamaguchi, T., Uemura, M., Maeshima, M., 2005. Identification of 33 rice aquaporin genes and analysis of their expression and function. Plant Cell Physiol. 46, 1568–1577.
Santiago-Tirado, F.H., Bretscher, A., 2011. Membrane-trafficking sorting hubs: cooperation between PI4P and small GTPases at the trans-Golgi network. Trends Cell Biol. 21, 515–525.
Santoni, V., Verdoucq, L., Sommerer, N., Vinh, J., Pflieger, D., Maurel, C., 2006. Methylation of aquaporins in plant plasma membrane. Biochem. J. 400, 189–197.
Scebba, F., Bernacchia, G., De Bastiani, M., Evangelista, M., Cantoni, R.M., Cella, R., Locci, M.T., Pitto, L., 2003. Arabidopsis MBD proteins show different binding specificities and nuclear localization. Plant Mol. Biol. 53, 715–731.
Schiestl, R.H., Petes, T.D., 1991. Integration of DNA fragments by illegitimate recombination in *Saccharomyces cerevisiae*. Proc. Natl. Acad. Sci. U.S.A. 88, 7585–7589.
Sebastiani, L., Scebba, F., Tognetti, R., 2004. Heavy metal accumulation and growth responses in poplar clones Eridano (*Populus deltoides* × *maximowiczii*) and I-214 (*P.* × *euramericana*) exposed to industrial waste. Environ. Exp. Bot. 52, 79–88.
Sheremet, I.A., Emets, A.I., Verbelen, J.P., Blium, I.B., 2009. The effect of okadaic acid on root morphology of *Arabidopsis thaliana* and microtubule organization in its cells. Tsitol. Genet. 43, 3–10.
Simonsen, A., Wurmser, A.E., Emr, S.D., Stenmark, H., 2001. The role of phosphoinositides in membrane transport. Curr. Opin. Cell Biol. 13, 485–492.
Singh, S., Parihar, P., Singh, R., Singh, V.P., Prasad, S.M., 2015. Heavy metal tolerance in plants: role of transcriptomics, proteomics, metabolomics, and ionomics. Front. Plant Sci. 6.
Stoláriková, M., Vaculík, M., Lux, A., Di Baccio, D., Minnocci, A., Andreucci, A., Sebastiani, L., 2012. Anatomical differences of poplar (*Populus* × *euramericana* clone I-214) roots exposed to zinc excess. Biologia 67, 483–489.
Tack, F., Vervaeke, P., Meers, E., Vandecasteele, B., 2005. Phytoremediation/stabilisation of dredged sediment derived soils with willow. Geophys. Res. Abstr. 7 08101–08101.
Tognetti, R., Sebastiani, L., Minnocci, A., 2004. Gas exchange and foliage characteristics of two poplar clones grown in soil amended with industrial waste. Tree Physiol. 24, 75–82.
Tuskan, G.A., Difazio, S., Jansson, S., Bohlmann, J., Grigoriev, I., Hellsten, U., Putnam, N., Ralph, S., Rombauts, S., Salamov, A., Schein, J., Sterck, L., Aerts, A., Bhalerao, R.R., Bhalerao, R.P., Blaudez, D., Boerjan, W., Brun, A., Brunner, A., Busov, V., Campbell, M., Carlson, J., Chalot, M., Chapman, J., Chen, G.-L., Cooper, D., Coutinho, P.M., Couturier, J., Covert, S., Cronk, Q., Cunningham, R., Davis, J., Degroeve, S., Déjardin, A., Depamphilis, C., Detter, J., Dirks, B., Dubchak, I., Duplessis, S., Ehlting, J., Ellis, B., Gendler, K., Goodstein, D., Gribskov, M., Grimwood, J., Groover, A., Gunter, L., Hamberger, B., Heinze, B., Helariutta, Y., Henrissat, B., Holligan, D., Holt, R., Huang, W., Islam-Faridi, N., Jones, S., Jones-Rhoades, M., Jorgensen, R., Joshi, C., Kangasjärvi, J., Karlsson, J., Kelleher, C., Kirkpatrick, R., Kirst, M., Kohler, A., Kalluri, U., Larimer, F., Leebens-Mack, J., Leplé, J.-C., Locascio, P., Lou, Y., Lucas, S., Martin, F., Montanini, B., Napoli, C., Nelson, D.R., Nelson, C., Nieminen, K., Nilsson, O., Pereda, V., Peter, G., Philippe, R., Pilate, G., Poliakov, A., Razumovskaya, J., Richardson, P., Rinaldi, C., Ritland, K., Rouzé, P., Ryaboy, D., Schmutz, J., Schrader, J., Segerman, B., Shin, H., Siddiqui, A., Sterky, F., Terry, A., Tsai, C.-J., Uberbacher, E., Unneberg, P., Vahala, J., Wall, K., Wessler, S., Yang, G., Yin, T., Douglas, C., Marra, M., Sandberg, G., Van de Peer, Y., Rokhsar, D., 2006. The genome of black cottonwood, *Populus trichocarpa* (Torr. & Gray). Science 313, 1596–1604.
Ueda, M., Tsutsumi, N., Fujimoto, M., 2016. Salt stress induces internalization of plasma membrane aquaporin into the vacuole in *Arabidopsis thaliana*. Biochem. Biophys. Res. Commun. 474, 742–746.
Vera-Estrella, R., Barkla, B.J., Bohnert, H.J., Pantoja, O., 2004. Novel regulation of aquaporins during osmotic stress. Plant Physiol. 135, 2318–2329.
Verdoucq, L., Rodrigues, O., Martinière, A., Luu, D.T., Maurel, C., 2014. Plant aquaporins on the move: reversible phosphorylation, lateral motion and cycling. Curr. Opin. Plant Biol. 22, 101–107.
Vitale, A., Hinz, G., 2005. Sorting of proteins to storage vacuoles: how many mechanisms? Trends Plant Sci. 10, 316–323.
Yamaguchi, H., Fukuoka, H., Arao, T., Ohyama, A., Nunome, T., Miyatake, K., Negoro, S., 2010. Gene expression analysis in cadmium-stressed roots of a low cadmium-accumulating solanaceous plant, *Solanum torvum*. J. Exp. Bot. 61, 423–437.
Zhang, Y., Wang, Z., Chai, T., Wen, Z., Zhang, H., 2008. Indian mustard aquaporin improves drought and heavy-metal resistance in tobacco. Mol. Biotechnol. 40, 280–292.
Zhao, F.J., Lombi, E., Breedon, T., M, S.P., 2000. Zinc hyperaccumulation and cellular distribution in *Arabidopsis halleri*. Plant Cell Environ. 23, 507–514.
Zheng, J., Han, S.W., Munnik, T., Rojas-Pierce, M., 2014a. Multiple vacuoles in impaired tonoplast trafficking3 mutants are independent organelles. Plant Signal. Behav. 9.
Zheng, J., Han, S.W., Rodriguez-Welsh, M.F., Rojas-Pierce, M., 2014b. Homotypic vacuole fusion requires VTI11 and is regulated by phosphoinositides. Mol. Plant 7, 1026–1040.
Zhu, J.K., 2016. Abiotic stress signaling and responses in plants. Cell 167, 313–324.